2004

# Crankshaft Bearing Analysis of a Single-Stage, Semi-Hermetic Carbon Dioxide Compressor

Beat Hubacher
*Purdue University*

Eckhard A. Groll
*Purdue University*

# CRANKSHAFT BEARING ANALYSIS OF A SINGLE-STAGE, SEMI-HERMETIC CARBON DIOXIDE COMPRESSOR

**Beat Hubacher* and Eckhard A. Groll**
Purdue University, School of Mechanical Engineering
Ray W. Herrick Laboratories, West Lafayette, Indiana 47907, USA

*Corresponding Author: beathubacher@alumni.purdue.edu

## ABSTRACT

This paper discusses the analysis of hydrodynamic journal bearings used in a semi-hermetic, reciprocating carbon dioxide compressor. The two journal bearings, which supported the crankshaft of the compressor, were greatly loaded due to the high pressures associated with the transcritical carbon dioxide cycle.

The study was initiated after a failure of one of the crankshaft bearings during performance testing. The semi-hermetic reciprocating compressor was equipped with two cylinders in a single-stage configuration. The compressor was an early prototype, which was originally used for air compression and re-designed for carbon dioxide compression. This is an important fact, since the bearing design was not significantly modified to handle the combination of high pressures and low oil film viscosities due to the dissolving of carbon dioxide in the refrigeration oil.

A friction loss analysis was conducted, which used previously obtained compressor performance data as inputs. In the first step, the force loads acting on the two crankshaft bearings were predicted based on the operating conditions. In the next step, the predicted force loads were used in the bearing loss analysis. It was found that the frictional losses of the two crankshaft bearings contribute with approximately 19 to 43 % to the total frictional losses depending on the operating conditions. In addition, it was found that the bearings were significantly loaded and thus, the oil film reduced to a critical minimum at which wearing effects become important. Based on these findings, a parametric study was conducted with the goal to identify bearing parameter values, which help to increase the oil film thickness. However, it was found that the oil film thickness of the hydrodynamic bearings of the investigated prototype compressor cannot be improved to satisfaction. It is suggested that other bearing concepts such as ball bearings should be used as an alternative to the hydrodynamic lubrication bearings for the given compressor design.

## INTRODUCTION

The transcritical $CO_2$-vapor compression cycle operates at very high pressures compared to fluorocarbon-based refrigerants. For example, the critical pressure of carbon dioxide is 7.38 MPa at a critical temperature of 31°C. This instant leads in carbon dioxide A/C-systems to discharging pressures of up to 14 MPa, which results in significantly higher force loads on the bearings of carbon dioxide compressors compared to fluorocarbon-based refrigerant compressors. In the study presented here, the crankshaft bearing losses of a semi-hermetic, reciprocating compressor with a two cylinder, single-stage configuration were investigated. In an earlier study by Hubacher et al. (2002), the experimentally measured performance of the same compressor using a hotgas-bypass compressor load stand was presented. The performance data from the previous study were then used in the present work as inputs for the bearing analysis. The compressor crankshaft was equipped with two hydrodynamic lubrication bearings, which were located in the middle and at the end of the shaft. The hydrodynamic lubrication principle is widely used for refrigeration compressors due to its reliability and durability. The rotating crankshaft is supported by the two journal bearings whereas the surfaces of the bearing bush and the journal are separated by an oil-film. The existence of such an oil film depends mainly on the relative velocity of the two surfaces, the shape, and the geometry of the bearing. Furthermore, a pressure field builds up in the oil film due to the load, which acts on the journal. In fact, a higher oil-film pressure can carry a higher load. The rotation of the joumal leads to a shearing of the oil-film, which generates friction losses. Therefore, it is important to reduce the friction losses by properly designing the bearing. However, it is even more important to guarantee a complete separation of the two friction surfaces. Since these surfaces are never absolutely smooth, the larger asperities of the two opposite surfaces start to touch and as a result, a significant increase of friction occurs. Hydrodynamic lubrication can be identified by four different lubrication regimes (Bhushan, 1999). When the surfaces are completely separated, full hydrodynamic lubrication takes place. This is

the ideal case, which should be achieved. For a smaller oil film thickness, elastohydrodynamic lubrication occurs where the oil film is still the main carrier of the bearing load. In contrast, the boundary lubrication regime is dominated by surface interactions during which wearing effects may occur, which significantly increase the friction losses. The transition regime between elastohydrodynamic lubrication and boundary lubrication is known as mixed lubrication where both effects can occur. As mentioned earlier, higher oil-film pressures are capable to carry higher loads, but are generally associated with very thin oil-films, which lead to elastohydrodynamic or boundary lubrication.

The transcritical carbon dioxide cycle generates very high bearing loads due to the high discharge pressures, which either requires a very large bearing or leads to a very thin oil-film in the bearing. The load carrying capacity of a bearing can be increased by increasing the viscosity of the lubricant. However, the friction losses increase at the same time. Due to the fact that carbon dioxide is dissolved into the lubricant, its viscosity decreases significantly due to the much lower viscosity of carbon dioxide.

## $CO_2$-COMPRESSOR BACKGROUND

It was reported by Hubacher and Groll (2003) that most of the early investigations on hermetic-type $CO_2$ compressors focused on the design issues associated with the use of $CO_2$ or the modification of existing HCFC-22 compressors to use with carbon dioxide. Furthermore, they reported that in more recent studies, prototype designs of hermetic compressors for use with carbon dioxide have been built and analyzed. Especially tribological studies in relation with the transcritical carbon dioxide were not very often addressed in the past, which is quite surprising since the high loads on the bearings in carbon dioxide compressors and the low viscosity evidently represent a significant problem, which is not as critical for fluorocarbon refrigerant compressors. The most comprehensive study on the design of modern carbon dioxide compressors was conducted by Suess (1998, 2002), who also discussed the bearing issue. He found that the fractional friction losses, which are the friction losses of a particular component compared to the total frictional losses as a percentage, are 34.7 % for the piston-cylinder assembly, 9.3 % for the piston pin bearing, 11.8 % for the linkage of the connecting rod and the crankshaft, 15.7 % for the crankshaft bearing, 11.2 % for the oil-pump, and 17.3 % for the shaft seal of the open-drive compressor. Furthermore, these values were presented for a single-stage, open-drive reciprocating compressor. In addition, Suess concluded that leakage can become a problem due to the large differential pressures across the compression stage. The author suggested the use of piston-rings to reduce the leakage. In Suess' opinion, a reciprocating compressor with a relatively short piston sealing path is the most promising concept for carbon dioxide compressors. Further, Suess reported that the piston-pin bearing is the most critical bearing of a carbon dioxide compressor due to the space limitation caused by the small bore. In fact, it is desired to realize a small bore in a carbon dioxide compressor since this linearly decreases the force load on the driving-mechanics. With respect to this issue, Suess found that based on his simulation a stroke-to-bore ratio of 1.2 to 1.6 is the most favorable to achieve high efficiencies. Finally, he rated the load on the crankshaft bearings of his investigated carbon dioxide compressor as feasible for a hydrodynamic lubrication bearing.

In summary, it was found that only little information on the hydrodynamic bearing load problematic of carbon dioxide compressors is available in the literature. Additional studies are needed to develop reliable and durable carbon dioxide compressors.

## OBJECTIVE

The present study was limited to the two crankshaft journal bearings of the given compressor, since one of these bearings failed. Both bearings are located inside the compressor shell: one is situated at the center of the crankshaft and the other is located at the end of the shaft. Figure 1 depicts a cross-sectional drawing of the compressor shell. The compressor is a single-stage, two-cylinder reciprocating compressor. The electric motor, the crankshaft, the connecting rods, the two crankshaft bearings, and the pistons are schematically illustrated in Figure 1. It can be seen that the electric motor is connected to the crankshaft, which is driven by the motor. The two connecting rods are linked to the crankshaft and pinned to the pistons so that they can transmit the motion. The two journal bearings that support the crankshaft are labeled as *Bearing D* and *Bearing E*. The bearing that failed during operation was bearing E. A more detailed drawing of the crankshaft is depicted in Figure 2. On the left of the figure is a design draw-

ing of the crankshaft with the bearings located on either side of the cranks. The connecting rod is depicted on the right hand side of the figure, while two arrows point to its linkage locations on the crankshaft. Hydrodynamic lubrication bearings maintain an oil film between the journal and the bearing bush surface whereby oil is lost at the edges of the bearing. This oil needs to be re-supplied to the bearing, which is realized by a channel labyrinth inside the crankshaft. The channels are indicated and labeled with *Oil Supply*. At the left end of the journal was an oil-pump hooked up to the crankshaft to supply the bearings with oil. The oil pump sucked the oil through an external oil-cooler to reduce the oil temperature as much as possible and provide the oil directly to the bearings. The oil cooler was used since at lower temperatures the viscosity of the oil is higher and thus, a better separation between the friction surfaces is guaranteed.

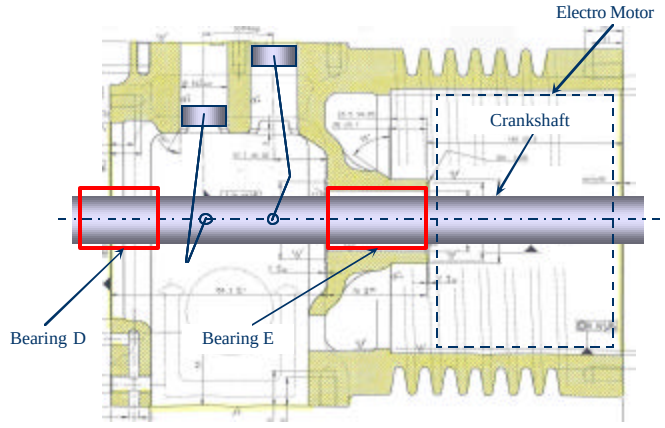


Figure 1: Cross-Section of compressor shell.

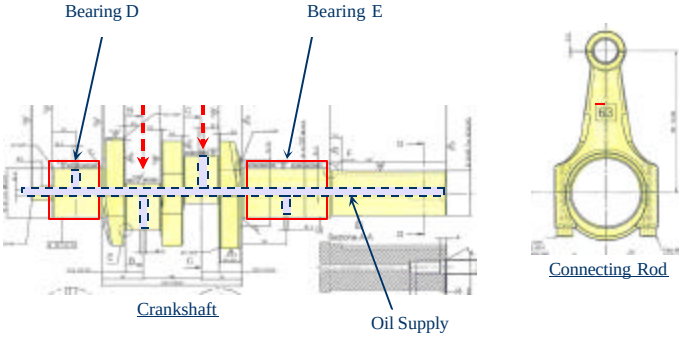


Figure 2: Crankshaft (left) and connecting rod (right).

The analysis presented in this work focused on the two journal bearings D and E. The bearing D has a width of 40 mm and a diameter of 45 mm, whereas the bearing E has a width of 50 mm and a diameter of 45 mm. The journal diameter at the bearing locations is 42.3 mm, which results in a bearing clearance of 1.35 mm. The bearing clearance is the distance between the two surfaces for a perfectly centered journal. In addition, the oil pump has an estimated oil flow rate of 0.08 kg/s.

## ANALYSIS

### Bearing Force Load

In a first step, the previously obtained and published compressor performance data (Hubacher et al., 2002) and the geometry data were taken to derive the cylinder pressure as a function of the crank angle. The displacement was evaluated relative to the crank angle by applying trigonometric relationships. Then, a polytropic process was applied by using a polytropic exponent, which was obtained from the measurements. The polytropic exponent $n$ was obtained as a function of the pressure ratio $pr$ from the measurement data:

$$n = a_0 + a_1 \cdot pr + a_2 \cdot \frac{1}{pr} + a_3 \cdot \left(\frac{1}{pr}\right)^2 \tag{1}$$

where $a_0$ to $a_3$ are fitted coefficients. In addition, the clearance volume was estimated based on the measured volumetric efficiencies, since the clearance volume was unknown. The volumetric efficiency is directly influenced by the clearance volume due to the fact that a larger clearance volume results in a larger re-expansion and thus, the volumetric efficiency decreases. Furthermore, the volumetric efficiency can be obtained theoretically using the following relationship:

$$h_{vol} = a - \frac{c_f}{1-c_f} \cdot \left[ pr^{1/n} - 1 \right] \tag{2}$$

where $c_f$ is the fractional clearance volume and $a$ is the offset from a volumetric efficiency of 1 for a pressure ratio of 1 due to the boundary effects such as leakage, internal superheating, and pressure losses across the valves. Equation (2) was fitted to the measured volumetric efficiency data and the fitting coefficients were obtained (see Figure 4). For the fractional clearance volume ($V_{min}/V_{max}$), a value of 0.115 was obtained. However, a fractional clearance

volume of 0.10 was finally used for further analysis. With this information and the cylinder volume as a function of the crank angle, the cylinder pressure was obtained using a polytropic process. Next, the force load on the piston was determined based on the fact that the cylinder pressure and the suction pressure act in opposite directions on the piston. Hence, the effective force load acting on the piston is the pressure difference of the cylinder and the suction pressure multiplied by the piston area. This force load acting on the piston was obtained for both cylinders whereby the forces are similar in magnitude, but 180 degree out-of-phase. Using Newtons 2nd law for force and momentum the force loads acting on the crankshaft bearings were obtained:

$$\sum F = m \cdot \ddot{x}\,, \quad \sum M_O = J_O \cdot \ddot{q}\,, \tag{3}$$

The force loads due to the force acting on the piston were defined by a right-handed Cartesian coordinate system in three dimensions. The force load information is crucial to obtain the frictional losses on the crankshaft bearings, to calculate the film thickness, and to determine the journal eccentricity with respect to the journal axis center.

## Bearing Friction Loss

The next step contained the analysis of the hydrodynamic journal bearings. The goal was to estimate the power losses due to friction, which are associated with the two crankshaft bearings. Therefore, the lubrication properties were estimated in a separate analysis based on the publication from Li and Rajewski (2000) on the oil properties of ISO 32 Alkyl Naphthalene (AN) and ISO 68 Polyol Ester (POE). The published data of the ester oil were modified to an ISO 100 Polyol Ester lubricant by shifting the viscosity curve at a temperature of 40 °C through a viscosity value of 100 cS instead of 68 cS. This approximation was taken as accurate enough for temperatures around 40 °C. Li and Rajewski (2000) reported the solubility as a function of pressure and temperature and furthermore, the kinematic viscosity as a function of temperature and solubility. The solubility was cast into an exponential function with the vapor pressure as the argument for a given temperature. The vapor pressure data for the given solubilities were provided by fitting the vapor pressure versus the temperature using the Clausius-Clapeyron equation (Seeton, 2000). The obtained function was then evaluated at the actual vapor pressure and the solubility was obtained as a result. In addition, the kinematic viscosity was fitted as a function of the temperature using Vogel's equation (Stachowiak and Batchelor, 2001) for three given solubility values. This regression was evaluated at the given temperature and kinematic viscosities for all three solubility levels were obtained. In the last step, the actual kinematic viscosity was obtained by first fitting an exponential function versus the three solubilities for a given temperature and then evaluating the new function using the effective solubility value.

The bearing friction loss was estimated using a regression equation (Stachowiak and Batchelor, 2001), which was derived from a sample of several hundred theoretically evaluated journal bearings. The regression equation takes the geometrical data, bearing operation data, and the viscosity data as arguments and delivers an estimation of the bearing power loss. The regression can be written as:

$$H = 3.9307 \cdot 10^{3} \cdot u_1^{-0.706} \cdot u_2^{1.577} \cdot L^{0.477} \cdot D^{2.240} \cdot N^{1.287} \cdot c^{0.249} \cdot T_s^{-0.204} \cdot \left(1 + \ln W^{*}\right)^{1.324} \tag{4}$$

## Oil film Thickness

The hydrodynamic journal bearing was analyzed with respect to its oil film thickness using the Reynolds equation, which is a simplified form of the Navier Stokes equations. The Reynolds equation was solved numerically and entirely non-dimensional whereby the only specification was the width-to-diameter ratio of the bearing. All of the other bearing data was applied to the non-dimensional results (Stachowiak and Batchelor, 2001). The non-dimensional solution was obtained only for a width-to-diameter ratio of bearing E (1.182), which is located at the crankshaft center. Since the specific force loads of the bearing D and E are very similar, only the lubrication film thickness of bearing E was studied. The purpose of this study was to investigate if the oil-film thickness was large enough to safely separate the two friction surfaces. The minimal oil film thickness plays an important role for hydrodynamic journal bearings, since a large squeezing of the oil film leads to a higher oil film pressure and thus, to a larger support capacity of the bearing. However, a certain oil film thickness needs to be maintained to still separate the asperities of the two friction surfaces. If this is not satisfied, the friction losses will drastically increase and wear effects can lead to a bearing failure. Figure 3 depicts a simplified illustration of a hydrodynamic journal bearing. A cross-section shows the bearing bush (outer circle) and the journal (inner circle). On the left side, the journal is rotating unloaded and its axis coincidences with the center position. That means that the distance from the journal surface to the bearing bush surface around the annulus is the same. This distance is called the bearing clearance *c*. On the right side, the journal is loaded with a force load *W*, which results in a squeezing of the oil film. Further-

more, the journal deviates from its center position by an eccentric distance $e$ as can be seen from Figure 3. As a result, the minimum oil film thickness reduces by the eccentric distance. This eccentric deviation can be expressed as a non-dimensional number. It is termed the eccentricity $e$ and is defined as:

$$e = \frac{e}{c} \tag{5}$$

where $e$ is the eccentric deviation from the center position of the bearing and $c$ is the bearing clearance. In addition, it needs to be noted that the minimum oil film thickness never exactly occurs at the force load line. It occurs slightly to the right of the force load line as illustrated in Figure 3. A loaded hydrodynamic journal bearing always operates with an eccentrically positioned journal so that a pressure can build up in the oil film. The eccentricity can take values between 0 and 1, while the former is a position with zero clearance and the latter is the center position with full clearance. However, an eccentricity of close to 1 indicates that the surfaces of the journal and the bearing already touch at the roughest surface locations. At that point, the oil film thickness is very small.

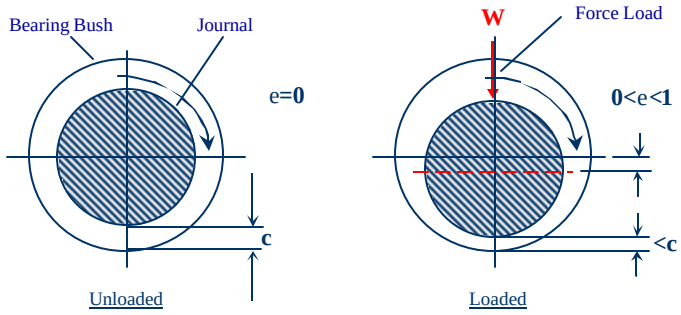


Figure 3: Schematic of hydrodynamic lubrication bearing.

In order to study the eccentricities, the 2D-Reynolds equation was solved numerically. Stachowiak and Batchelor (2001) presented in their book a complete Matlab code entitled "Partial" to solve the 2D-Reynolds equation. This code was implemented in Matlab and used to study the eccentricity relations. In a first approach, the code was run for different eccentricities between 0.1 and 0.9997. The problem becomes highly non-linear towards eccentricities of 1. Therefore, the mesh was gradually increased from 20x20 to 100x20, where the finer mesh width was chosen for the radial direction. The non-dimensional load by Stachowiak's notation is defined as:

$$W^* = \frac{W \cdot c^2}{6 \cdot h \cdot U \cdot L \cdot R^2} \tag{6}$$

## RESULTS

The hydrodynamic journal bearing analysis was carried out for six different cases where the cases 1 to 3 used the POE-oil and the cases 4 to 6 used the AN-oil. Furthermore, the suction pressures were set to 1.8 MPa for the cases 1 and 4, to 3.3 MPa for the cases 2 and 5, and to 4.8 MPa for the cases 3 and 6, respectively. The discharge pressure was always constant at 13.8 MPa, since this was the highest discharge pressure during the testing. The speed was specified as 1740 $min^{-1}$ and the superheat in the suction line was set to 10.7 K. Figure 5 shows the obtained P-V diagrams for the cases 4 to 6. It can be assumed that the P-V diagrams of the cases 1 to 3 are similar, since the different oils will have only minor influences on the shape of the P-V diagrams. Furthermore, it was found that the intermediate cases (2 and 5) generate the highest mean force loads on the bearings due to the shape of the P-V diagram. In fact, the mean net pressure difference, which is the averaged pressure difference between the cylinder pressure and the suction pressure during one cycle, is the largest for the intermediate suction pressure (3.3 MPa). Figure 6 shows the mean force loads for the bearings D and E for all six cases. Similarly to the P-V diagrams, the mean force loads show no differences between the two oils. The mean force loads have a magnitude of approximately 2500 N for the bearing D and approximately 3500 N for the bearing E. The force load differences between the minimum and maximum values due to the different suction pressures are not larger than 6 %, which shows that the force load does not significantly depends on the operating conditions. As will be seen later, this is not true for the friction losses of the bearing due to the changing oil properties. As mentioned before, the friction losses of the two bearings were determined by using Equation (4). The results are depicted in Figure 7. The friction losses are largest for the cases 3 and 6. The higher suction pressure led to a higher solubility and thus, to a lower viscosity. Furthermore, the high loads on the bearing caused small oil film thicknesses and led to elastohydrodynamic or mixed lubrication where wearing effects also take place. Additionally, the ratio of the bearing frictional loss to the total frictional loss was calculated and is depicted in Figure 8. The two bearings together contribute by up to 43 %

of the total frictional losses when using the POE-oil and by up to 19 % for the AN-oil. In fact, the lower viscosities of the POE-oil caused a thinner oil film and thus, more wearing effects, which finally led to the failure of the compressor.

The dimensionless friction load was obtained according to Equation (6) for a width-to-diameter ratio of 1.182, which corresponds to bearing E. A functional relationship between this dimensionless friction load and the bearing eccentricity was derived and is shown in Figure 9. The actual and optimum cases are depicted with arrows. The optimum eccentricity is around 0.75, which corresponds to a dimensionless friction load of approximately 1. Contrarily, the actual predicted dimensionless friction loads for the given compressor range from 442 to 1465, which reflects eccentricities close to 1. The exact results all of the six previously defined cases are listed in Table 1. The first two rows list the friction losses of the bearing D and E in [W]. In the additional rows, the supply oil temperature, the journal eccentricity, the effective and dimensionless force load on the bearing E, and the oil properties are listed. It can be seen from these results that the kinematic viscosity reduced significantly from the initial value of 100 cS at temperatures around 40 °C to values between 8 and 28 cS due to the high solubility of $CO_2$ in the oil of 3 to 24 %. The solubility was generally higher for the POE-oil than for the AN-oil. The significant reduction of the viscosity due to the high solubility of $CO_2$ is part of the problem of the hydrodynamic lubrication bearings and results in the reported eccentricities of close to 1. For instance, the minimum oil film thickness in case 4 was calculated as 0.88 µm, whereas the doubled surface roughness was assumed with 0.4 µm. This means that the separation of the two friction surfaces is extremely small. Similar situations were found for the other cases.

This work also studied the improvement of the actual bearing design by reducing the dimensionless force load on the bearing according to Equation (6). For this purpose, the force load and the bearing clearance were reduced, and the viscosity, the bearing width, and the journal radius were increased. The relative velocity between the two friction surfaces is a function of the radius and the rotational speed and thus, cannot be modified independently. The results of this study are listed in Table 2, where $f$ is the modification factor. A value of $f$ =1 represents the actual case. The actual case is shown in the first row of Table 2. The next row represents the case in which the parameters were adjusted by 20 % with the result that the dimensionless force load was reduced from 660.9 to 57.8. In the last row, the parameters were modified by 30 % and thus, the dimensionless force load was reduced to 32.1. In both cases, it was assumed that the viscosity of the lubricant was increased by a factor of 3, which can only be achieved by using new oils or by a significant reduction of the oil supply temperature. As can be seen from Figure 9, a dimensionless force load of 32.1 still equals an eccentricity of approximately 0.98 instead of the desired 0.75. Thus, even adjusting the bearing characteristics by 30 % and increasing the viscosity by a factor of 3, a satisfactory operation of the hydrodynamic journal bearing of the given compressor cannot be guaranteed. However, the curve in Figure 9 flattens out between a dimensionless force load of 32 and 1, which indicates that a further reduction of the dimensionless force load leads to a significant reduction of the eccentricity and possibly to satisfactory operation. It has to be noted that the reduction in the effective force load was achieved by a reduction of the cylinder bore.

## CONCLUSIONS

The analysis of the hydrodynamic journal bearing proved that the force loads acting on the journal bearing of the given $CO_2$-compressor are factors higher than for a conventional fluorocarbon-based refrigerant compressor. For example, a transcritical $CO_2$-compressor experiences about five times more force load on the bearings than a typical R-22 compressor. The analysis obtained results, which showed larger friction losses for the POE-oil compared to the AN-oil. The crankshaft bearing friction losses account for 19 to 43 % of the total frictional losses, which compares quite well to the study presented by Suess (1998). The analysis revealed that the reduction of the friction losses is not the primary concern of the given compressor. Instead, the main concern is that the large bearing overload can cause bearing failures at any time. This is due to the reason that the high loads greatly squeeze the oil film and thus, result in very thin films. Eccentricities of the journal were found to be close to 1, which means that the oil film reduces to a critical minimum and the journal touches the bearing surface. It can be concluded that the use of hydrodynamic lubrication for transcritical $CO_2$-applications is a critical issue and not necessarily a good choice. However, different design concepts and compressor configurations, e.g., two-stage compression where the crankcase shell is at intermediate pressure, can reduce the high bearing force loads and lead to less critical bearing situations. In addition, the authors recommend the study of other bearing types than the commonly used hydrodynamic lubrication bearing for the use in the transcritical carbon dio xide compressors.

## NOMENCLATURE

| | | | | | |
|---|---|---|---|---|---|
| $a_0 \ldots a_3$ | Fitting coeffic ients | [-] | $H$ | Frictional losses of bearing | [W] |
| $a$ | Offset parameter for vol. efficiency | [-] | $T$ | Oil supply temperature | [°C] |
| $pr$ | Pressure ratio | [-] | $D$ | Journal diameter | [-] |
| $n$ | Polytropic exponent for comp. process | [-] | $u_1$ | Kinematic viscosity at 37.8°C | [cS] |
| $c_f$ | Fractional clearance volume | [-] | $u_2$ | Kinematic viscosity at 93.3°C | [cS] |
| $e$ | Eccentricity of bearing journal | [-] | $V_{min}$ | Clearance volume of cylinder | [$m^3$] |
| $e$ | Journal deviation at the force line | [m] | $V_{max}$ | Total cylinder volume | [$m^3$] |
| $c$ | Bearing clearance | [m] | $F$ | Force | [N] |
| $W$ | Force load on bearing | [N] | $m$ | mass | [kg] |
| $W^*$ | Dimensionless force load on bearing | [-] | $\ddot{x}$ | Acceleration of mass | [$m/s^2$] |
| $U$ | Relative surface velocity | [m/s] | $M_O$ | Momentum | [Nm] |
| $L$ | Bearing width | [m] | $J_O$ | Moment of inertia | [kg-$m^2$] |
| $R$ | Journal radius | [m] | $\ddot{q}$ | Angular acceleration of crankshaft | [$rad/s^2$] |
| $h$ | Dynamic viscosity of lubricant | [Pas] | | | |

## REFERENCES


Bhushan, B., "Principles and Applications of Tribology", Wiley, New York, 1999.

Hubacher, B, Groll, E. A., and Hoffinger, C., "Performance Measurement of a Semi-Hermetic Carbon Dioxide Compressor", Proc. Int'l Refrig. Conf. at Purdue, West Lafayette, IN, July 16-19, pp. 477-485, 2002.

Hubacher, B., Groll, E. A., "Performance Measurement of a Hermetic, Two-Stage Carbon Dioxide Compressor", Proc. 2003 Int'l Congress of Refrig. (IIR), Washington, D.C., August 17-22, 2003.

Li, H., and Rajewski, T. E., "Experimental Study of Lubrication Candidates for the $CO_2$ Refrigeration System", Proc. of the 4th IIR–Gustav Lorentzen Conference., Purdue University, West Lafayette, IN, July 25-28, 2000.

Seeton, C., Fahl, J., and Henderson, D., "Solubility, Viscosity, Boundary Lubrication and Miscibility of $CO_2$ and Synthetic Lubricants", Proc. 4th IIR–Gustav Lorentzen Conf., Purdue, West Lafayette, IN, July 25-28, 2000.

Stachowiak, G. W., and Batchelor, A. W., "Engineering Tribology", 2nd ed, Butterworth-Heinemann, Boston, 2001.

Suess, J., "Low Capacity Hermetic Type Compressor for Transcritical CO2 Applications", Proc. Int. Compressor Eng. Conference, Purdue University, West Lafayette, 2002.

Suess, J., "Untersuchungen zur Konstruktion moderner Verdichter für Kohlendioxid als Kältemittel", PhD-Thesis, DKV, Stuttgart (Germany), pp. 149, 1998.


## APPENDICES

Table 1: Results from bearing D and E

| | Units | Case 1 | Case 2 | Case 3 | Case 4 | Case 5 | Case 6 |
|---|---|---|---|---|---|---|---|
| $H_D$ | [W] | 111.2 | 162.1 | 299.5 | 79.8 | 95.2 | 133.5 |
| $H_E$ | [W] | 126.0 | 183.1 | 338.1 | 90.5 | 107.6 | 150.9 |
| $T_{suc,intern}$ | [°C] | 47.04 | 47.80 | 44.56 | 47.30 | 48.08 | 44.78 |
| ε | [-] | 0.9988 | 0.9993 | 0.9995 | 0.9991 | 0.9993 | 0.9994 |
| W | [N] | 3357 | 3467 | 3273 | 3357 | 3467 | 3273 |
| W* | [-] | 442.1 | 739.2 | 1465 | 660.2 | 844.7 | 1058 |
| η | [Pas] | 0.02676 | 0.01653 | 0.00788 | 0.01792 | 0.01446 | 0.01090 |
| ν | [cS] | 28.17 | 17.41 | 8.28 | 18.11 | 14.62 | 11.01 |
| Solubility | [-] | 0.098 | 0.147 | 0.239 | 0.032 | 0.054 | 0.100 |

Table 2: Case study of bearing E (Case 4)

| $f_0$ | W | $f_1$ | c | $f_2$ | R | U | $f_3$ | L | $f_4$ | η | W* |
|---|---|---|---|---|---|---|---|---|---|---|---|
| [-] | [N] | [-] | [m] | [-] | [m] | [m/s] | [-] | [m] | [-] | [Pas] | [-] |
| 1.00 | 3357 | 1.00 | 0.00135 | 1.00 | 0.0212 | 3.9 | 1.00 | 0.050 | 1.00 | 0.0179 | 660.9 |
| 0.85 | 2853 | 0.80 | 0.00108 | 1.20 | 0.0254 | 4.6 | 1.20 | 0.060 | 3.00 | 0.0537 | 57.8 |
| 0.85 | 2853 | 0.70 | 0.00095 | 1.30 | 0.0275 | 5.0 | 1.30 | 0.065 | 3.00 | 0.0537 | 32.1 |

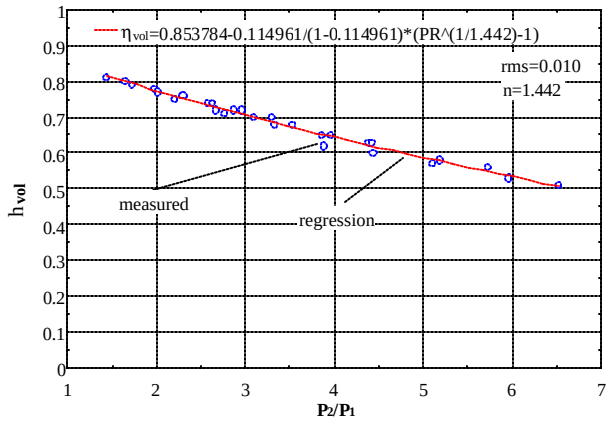


Figure 4: Fitting of volumetric efficiency.

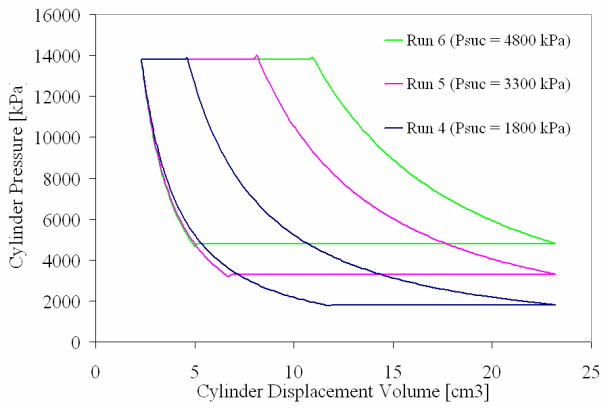


Figure 5: P-V-diagrams for three standard cases.

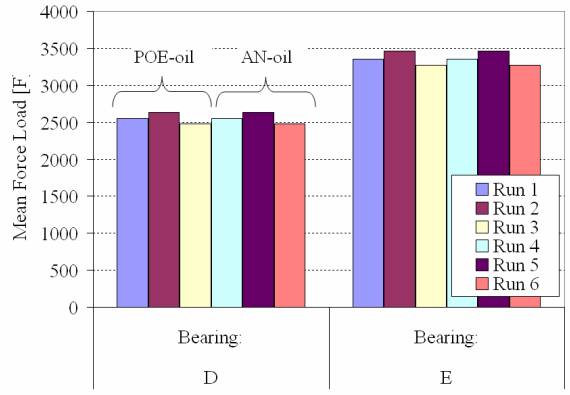


Figure 6: Mean force loads for both oils.

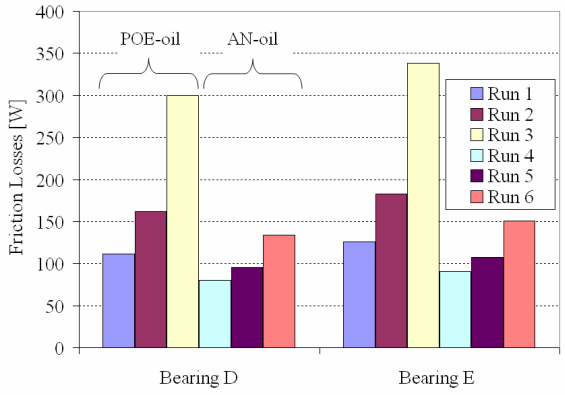


Figure 7: Friction losses for both oils.

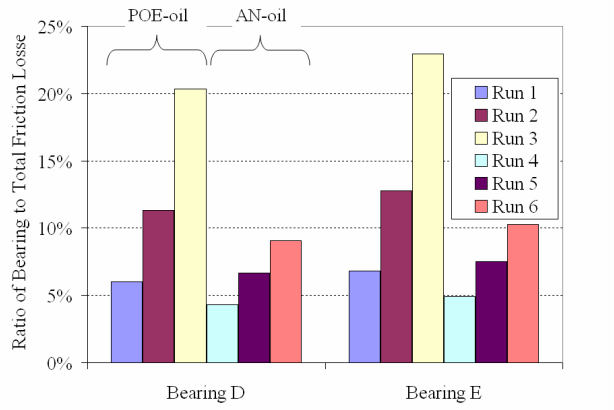


Figure 8: Percentile friction losses

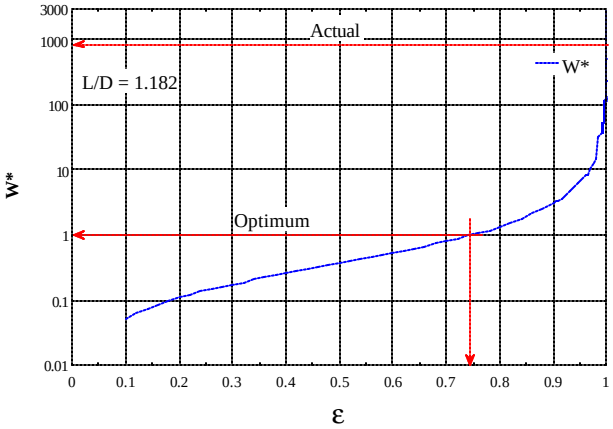


Figure 9: Non-dimensional force load vs. eccentricity